TGF-β Signaling Plays a Pivotal Role During Developmental Biliary Atresia in Sea Lamprey (*Petromyzon marinus*)

Yu-Wen Chung-Davidson [iD] ,[1] Jianfeng Ren,[2] Chu-Yin Yeh,[3] Ugo Bussy,[1] Belinda Huerta,[1] Peter Joseph Davidson,[1] Steven Whyard,[4] and Weiming Li[1]

Biliary atresia (BA) is a rare neonatal disease with unknown causes. Approximately 10% of BA cases develop in utero with other congenital defects that span a large spectrum of disease variations, including degeneration of the gall bladder and bile duct as well as malformation of the liver, intestines, and kidneys. Similar developmental alterations are manifested in a unique animal model, the sea lamprey (*Petromyzon marinus*), in which BA occurs naturally during metamorphosis. With the likelihood of conserved developmental mechanisms underlying organogenesis and degeneration, lamprey developmental BA may be a useful model to infer mechanisms underlying human embryonic BA. We reasoned that hepatobiliary transcriptomes regulate the transition between landmark stages of BA. Therefore, we examined sea lamprey hepatobiliary transcriptomes at four stages (M0, metamorphic stage 0 or larval stage, no BA; M2, metamorphic stage 2, onset of BA; M5, metamorphic stage 5, BA, and heightened hepatocyte proliferation and reorganization; and JV, juvenile, completion of BA) using messenger RNA sequencing and Kyoto Encyclopedia of Genes and Genomes pathway analyses. We found gene-expression patterns associated with the transition between these stages. In particular, transforming growth factor β (TGF-β), hedgehog, phosphatidylinositol-4,5-bisphosphate 3-kinase-Akt, Wnt, and mitogen-activated protein kinase pathways were involved during biliary degeneration. Furthermore, disrupting the TGF-β signaling pathway with antagonist or small interfering RNA treatments at the onset of BA delayed gall bladder and bile duct degeneration. *Conclusion:* Distinctive gene-expression patterns are associated with the degeneration of the biliary system during developmental BA. In addition, disrupting TGF-β signaling pathway at the onset of BA delayed biliary degeneration. (*Hepatology Communications* 2020;4:219-234).

Biliary atresia (BA), a rare infant disease with unknown causes, is characterized by fibrosclerosing cholangiopathy, resulting in obstruction or obliteration of extrahepatic bile ducts (EHBDs) and intrahepatic bile ducts (IHBDs).[1] In the United States, BA affects 1 in 8,000 to 20,000 neonates, with 250 to 400 new cases reported every year.[2] Approximately 10% of BA cases are embryonic form

with various laterality defects and the worst prognosis.[3] The most common congenital anomalies are BA splenic malformation syndrome with polysplenia, midline liver, intestinal malrotation, and complex cardiac malformations.[3,4] Some cases of embryonic BA can be diagnosed by small gall bladder (GB) or nonvisualization of GB in the second trimester on the prenatal sonographic scan.[5] In some cases of "cystic" BA, the bile duct cysts and GB contained a clear or whitish liquid without bile. These children had normal birth weight, were not jaundiced, and did not require liver transplantation at 5 years of age.[4] These diverse variations in biliary phenotypes and disease outcomes accentuate the need to understand the developmental causes of embryonic BA for better diagnosis and treatment strategies.

Youson and Sidon described naturally occurring developmental BA in sea lamprey during seven stages of metamorphosis.[6-8] The GB degenerated between M2 and M3 (Fig. 1), and bile ducts are almost always obliterated from M3 to M5. Rarely, one or two bile ducts remain at M6 to M7. The liver, intestine, and kidneys also undergo remodeling and reorganization throughout M3 to M7. The degenerative processes at various stages of lamprey developmental BA are similar to those observed in some clinical manifestations of human embryonic BA. Because metamorphosis is considered an extension of embryonic development and with the likelihood of conserved organogenesis and degenerative processes underlying GB, liver, kidney, and intestinal transformation, lamprey developmental BA may be a useful model to understand the mechanisms underlying embryonic BA.[6-9]

We reasoned that hepatobiliary transcriptomes at different stages of BA would be associated with the developmental transitions among these stages (Fig. 1).

Therefore, we examined sea lamprey hepatobiliary transcriptomes of larvae (M0: no BA) and at three landmark stages during developmental BA (M2: onset of BA and GB degeneration; M5: bile duct degeneration with heightened hepatocyte proliferation and reorganization; and newly transformed juvenile (JV): completion of BA and hepatocyte remodeling) using messenger RNA-sequencing (mRNA-seq) and Kyoto Encyclopedia of Genes and Genomes (KEGG) pathway analyses. The gene-expression patterns showed that the transforming growth factor β (TGF-β) signaling pathway intersected with multiple other developmental pathways, such as hedgehog, Wnt, and mitogen-activated protein kinase (MAPK) pathways, and each pathway exhibited changes in gene expression throughout the developmental processes. Subsequently, we perturbed the TGF-β signaling pathway at the onset of BA, resulting in distinctive biliary degeneration patterns and phenotypes in sea lamprey. Our results indicate possible mechanisms underlying developmental BA, which may provide testable hypotheses to infer etiologies of human embryonic BA.

Materials and Methods

COLLECTION AND MAINTENANCE OF ANIMALS

Sea lamprey larvae were collected by the staff of U.S. Geological Survey, Great Lakes Science Center, Hammond Bay Biological Station, or by the survey crew of U.S. Fish and Wildlife Service, Ludington Biological Station (Ludington, MI), and were kept in plastic tanks (98 × 54 × 48 cm^3) with flow-through

ARTICLE INFORMATION:

From the [1]Department of Fisheries and Wildlife, Michigan State University, East Lansing, MI; [2]Key Laboratory of Exploration and Utilization of Aquatic Genetic Resources, College of Fisheries and Life Sciences, Shanghai Ocean University, Shanghai, China; [3]College of Osteopathic Medicine, Michigan State University, East Lansing, MI; [4]Department of Biological Sciences, University of Manitoba, Winnipeg, MB, Canada.

ADDRESS CORRESPONDENCE AND REPRINT REQUESTS TO:

Weiming Li, Ph.D.
Department of Fisheries and Wildlife
Michigan State University
Natural Resources Building

480 Wilson Road, Room 13
East Lansing, MI 48824
E-mail: liweim@msu.edu
Tel.: +1-517-432-6705
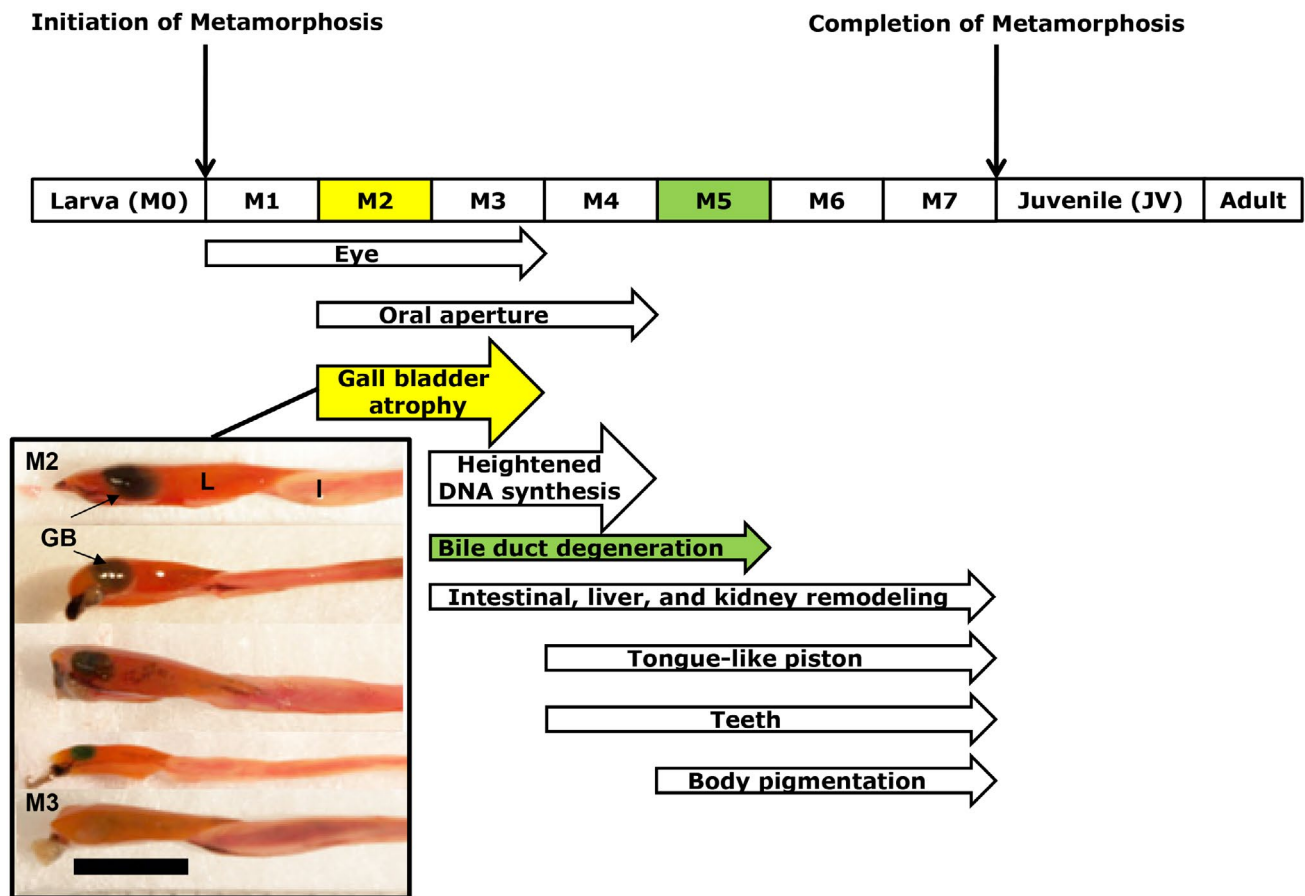
FIG. 1. Major developmental events occur during sea lamprey metamorphosis. Photographs demonstrate different degrees of GB degeneration (black arrows) during the transition from metamorphic stage 2 (M2) to 3 (M3). GB atrophy and bile duct degeneration, the major events at M2-M3 and M3-M5, are highlighted with yellow and light green, respectively. Scale bar: 5 mm. Abbreviations: I, intestine; L, liver; M0, larval stage; M1-M7, metamorphic stages 1-7.

water at 10 L/minute and 16°C ± 1°C. The bottom of the tanks were filled with 13 cm of fine sand, which can pass through No. 18 (1 mm), 3φ (125 μm), or 4φ (62.5 μm) U.S. standard sieve. Water was aerated with stone air breakers to keep dissolved oxygen levels near saturation. Larvae were fed with dried brewer's yeast (60 g/100 larvae, suspended in 100 mL water before use) once per week. M2 larvae that had started metamorphic processes stopped feeding and were checked every other week. Liver samples (including bile ducts and GB) were collected from various metamorphic stages, determined according to the appearance of eyes, the structure of oral aperture, the development of tongue-like piston, the cornification of teeth, and the coloration of the body.[7] Due to the difficulty of obtaining metamorphic larvae (M3-M7), sample sizes

varied among experiments (n = 2~40). All animals received humane care according to the criteria outlined in the *Guide for the Care and Use of Laboratory Animals* prepared by the National Academy of Sciences and published by the National Institutes of Health (NIH publication 86-23, revised 1985). Animal handling procedures were approved by the Institutional Animal Care and Use Committee at Michigan State University (MSU).

TRANSCRIPTOME ANALYSES

Total RNAs of pooled liver samples from different developmental stages (M0, M2, M5, and JV; five per stage) were extracted using TRIzol Reagent (Invitrogen/Thermo Fisher Scientific, Madison, WI)

and treated with TURBO DNA-free kit (Invitrogen) as described.[10] RNA samples (2 μg/sample) were enriched by the mRNA-seq 8 sample Prep Kit, and the transcriptomes were obtained using an Illumina Genome Analyzer II (San Diego, CA) and mRNA-seq protocol (75-mers; Illumina) at the Genomics Technology Support Facility at MSU. These sequences were trimmed with Trimmomatic-0.30 software, filtered for polynucleotides (more than 36 nt) with in-house Perl script, and aligned to the sea lamprey reference genome using TopHat software.[10-12] Gene-expression analysis of mRNA-seq was based on the gene model of *Petromyzon marinus* (Pmarinus_7.0.66).[11] Calculation of gene expressions (fragments per kilobase of transcript per million mapped reads) and identification of differentially expressed genes between different samples were performed using Cufflinks package v2.1.135.[13] Gene Ontology enrichment was performed using agriGO.[14,15] Ortholog assignment and pathway mapping were performed using Kyoto Encyclopedia of Genes and Genomes Automatic Annotation Server on the KEGG website (http://www.kegg.jp/). Sequence motifs for the TGF-β/mothers against decapentaplegic (SMAD) response elements (T/SREs) were GAGTTGGTGC, GTCTAGAC, CAG(A)$_{12}$, GCC(G)$_{12}$, and CCCGCCTCCT.[16-18]

REAL-TIME QUANTITATIVE POLYMERASE CHAIN REACTION

TaqMan minor groove binder (MGB) or SYBR Green system (Invitrogen) was used as described.[10] Briefly, total RNAs were reverse-transcribed into complementary DNA (cDNA) using Moloney murine leukemia virus reverse transcriptase (Invitrogen) and random hexamers (Promega Corp., Madison, WI) according to the manufacturer's protocols. Each quantitative real-time polymerase chain reaction (RT-PCR) consisted of 2 μL cDNA (5 ng/μL for TaqMan or 20 ng/μL for SYBR Green); 8 μL TaqMan or SYBR Green Universal PCR master mix containing 900 nM each forward and reverse primers; and 250 nM TaqMan MGB probe (for TaqMan only). Amplification plots were analyzed on an ABI 7900 quantitative RT-PCR thermal cycler (Applied Biosystems/Thermo Fisher Scientific, Foster City, CA). Synthetic oligos were used as standards and run simultaneously on the same plate. The sequences

for the standard oligos, primers (underlined), and TaqMan probes (bold) were as follows.

TGF-β1:

5′<u>CTGCCTCCGCCACCTCTACATA</u>**AACTTCCGTAAGGACCTG**GGATG<u>GAACTGGATCCACGAGCCC</u>3′

TGF-β2:

5′<u>GCACTGGCGCCACTTATGTCC</u>**CTGTCTATGTTGAACTTC**T<u>TTTTTCGCACCGTGCATAGC</u>3′

TGF-β receptor I (TGF-βRI):

5′<u>CTGCACATTGTGGCCAAGATCA</u>**TGCAGGAGTGTTGGTAC**C<u>ACAACGCAGCGGCTCG</u>3′

TGF-β receptor II (TGF-βRII):

5′<u>TGAAGGAGTACTGGCTCATCACA</u>GCGTACCACCCGCGGGG**AAACCTGCAGGACCTGA**TCATGCGCAAGGTGCTGAGCTGGCGCG<u>AGCTAATGCTGCTGGGCG</u>3′

SMAD1:

5′<u>GCTGCAGCCTCAAGATCTTCAA</u>**CAACCAGGAGTTTGCGG**G<u>CCTGTTGGCCGAGTCTGTGAA</u>3′

SMAD2:

5′<u>GAGCTACGCGCCATCGAC</u>**TGCTGTGAATTCGCCT**TCAACC<u>TCAAGAAGATGGAGGTGTGCG</u>3′

SMAD3:

5′<u>CCGCATGAGCTTCGTCAAAGGCT</u>GGGG**TGCCGAGTACAGGCGT**CAGA<u>CGATCACGAGCACACCGT</u>3′

SMAD4:

5′<u>TCGGCCAGCTCTCCAATGT</u>**TCATCGGACTGATGCCA**G<u>CGAAAAGGCGAGGCAAGTAC</u>3′

SMAD6:

5′<u>TCACCAGATGCCATGAAGCAG</u>CCCTGC**TGGTGCCACGTAGCGT**ACTGGGAACACCGCTCTCGAGTCGGGCGCCTGTACCCTGTGGGCGACGCT<u>TCAGTGGCTGTCTTCTACGACCT</u>3′

SMAD7:

5′<u>TTCTGTGCCGGCTATTTCGCTGGC</u>**CAGATGTGCGGCACCA**GAGG<u>GAACTCAAGCGCCTCTGCTG</u>3′

Cytochrome P450 7A1 (CYP7A1):

5′<u>CAACATGTCGGCGCTCATCGC</u>**CCTCCGAATACAACTCA**A<u>TGACACGCTGTCTCGCATG</u>3′

CYP27A1:

5′<u>TCTGGCCAAAATGTCATTCCTT</u>**AAGG
CTGTCATCAAAG**AGATTC<u>TCAGACTGTATC
CAGTGGTGCC</u>3′

Hepatocyte Growth Factor Receptor (MET):

5′<u>CTGCAGACGCAGAGGTTCACC</u>**ACCA
AGTCGGATGTGTG**G<u>TCGTTTGGCGTTCT
GCTG</u>3′

Nitric Oxide Synthase 2 (NOS2):

5′<u>AGCGCACAGTGACATTGTTT</u>ATCTC
ACGTAGATGTA**TGCAGCGCCTTGTTCTC
AAGCGC**TTTAACCAACAGCGACAGGAT
TTGCATGCGATGATAAGTGGTTGAGAT
AAATAGCTGAGTGGGGGTTGGTAAAAGT
GGTGGTGCAGTTGCGGTGACAGGAG
<u>GACAGGTGCTAGAGA</u>3′

Caspase-7: 5′<u>AGGAATAGCTCGCAGTTGGA</u>
GCTCGTGAAGATAC**TCGTGTGCGTGA
ACCGCCGC**GTGGCCACGCAGTACGTGTC
CTGCTCACGGGACATCACCTACAACGA
<u>CAAGAAGCAGATTCCGTGCA</u>3′

B-Cell Lymphoma 2:

5′<u>TGACCTTGTAAGTGCGACCTA</u>ATC
GGTTGTGACCGGCGAATGCGACGA
CGACGTTGCAGGCACCAATAGCGGGTCC
AT**GACGAGCTCGGCGCATCGCG**ATT
GCGTGGAGGTGGACCCCGATTGGA
TGGAGACGCACGAG<u>AGGATCAACAATG
CCGAGGA</u>3′

ULTRA-HIGH-PERFORMANCE LIQUID CHROMATOGRAPHY–TANDEM MASS SPECTROMETRY

Bile acid analyses were modified from previously developed methods.[19] Briefly, liver samples were weighed, homogenized in 1 mL of 75% ethanol, and incubated overnight in a shaker (70 rpm) at room temperature. Samples were centrifuged at 15,800g, 4°C for 20 minutes twice, and the supernatant was freeze-dried overnight and reconstituted in 1 mL of 50% methanol. The ultra-high-performance liquid chromatography–tandem mass spectrometry (UPLC/MS-MS) system consisted of a Waters ACQUITY H-Class UPLC system connected to a Waters Xevo TQ-S triple quadrupole mass spectrometer (Milford, MA). The mobile phase consisted of water (containing 10 mM triethylenetetramine) as solution A and methanol as solution B. A Waters ethylene bridged

hybrid C18 column (2.1 mm × 50 mm, 1.7 μm particle size), coupled with an ACQUITY UPLC column in-line filter kit (0.2 μm filter), was used. Separation was achieved using the following gradient program at a flow rate of 250 μL/minute for 12 minutes at 35°C: 60% A for 2 minutes, decreased to 20% A from 2 to 7 minutes, decreased to 0% A from 7 to 7.01 minutes, maintained at 0% A from 7.01 to 9.00 minutes, increased to 60% A from 9.0 to 9.01 minutes, and maintained at 60% A to 12 minutes for column equilibrium. The injection volume was 10 μL.

TGF-βRI ANTAGONIST SJN2511 EXPERIMENT

M2 larvae were injected with 0.05% dimethyl sulfoxide (DMSO) (vehicle control; n = 40) or RepSox (SJN2511; Tocris Bioscience, Minneapolis, MN; 7.183 ng/g body weight, equivalent to 0.025 μM dissolved in 0.05% DMSO; n = 40) intraperitoneally. After 10 days, animals were euthanized and morphological changes were recorded. Liver samples were snap-frozen in liquid nitrogen for quantitative RT-PCR (n = 10 × 1 set and 8 × 3 sets) and UPLC/MS-MS (n = 6). The animals were treated for 10 days because it took 1 to 2 weeks for the M2 larvae to progress to M3.[7]

SMALL INTERFERING RNA EXPERIMENT

Stealth RNA interference (RNAi) small interfering RNAs (siRNAs) were designed using the online BLOCK-iT RNAi Designer (https://rnaidesigner.thermofisher.com/rnaiexpress/) and ordered from Life Technologies/Thermo Fisher Scientific (Grand Island, NY). A total of 56 M2 larvae were injected with 0.3 mM TGF-β1 siRNA, TGF-βRII siRNA, or their respective control siRNA (CI: scrambled sequence of TGF-β1 siRNA; CII: scrambled sequence of TGF-βRII siRNA) in 3.3% lipofectamine (Life Technologies) intraperitoneally (n = 14 for each group; see below for lists of sequences). Liver samples from each treatment group were collected 4 days after treatment and snap-frozen for quantitative RT-PCR (eight samples/treatment group) and bile acid UPLC/MS-MS analyses (six samples/treatment group). Four-day treatment was determined by a preliminary time-course experiment showing that siRNA was effective

from 3 hours to 4 days after injection. An additional 30 M2 larvae were injected with vehicle (3.3% lipofectamine), 0.3 mM TGF-β1 siRNA, or TGF-βRII siRNA intraperitoneally (n = 10 for each group). Liver samples were collected 2 weeks after treatment and fixed in hydrogel for CLARITY and immunofluorescent confocal microscopy imaging.[10,20] Two-week treatment was chosen because it took 1 to 2 weeks for M2 larvae to progress to M3.[7] Note that some animals died before sample collection.

TGF-β1 siRNA: 5′CAAUGGUGAGUUGUGUGUCUUUGUU3′

CI: 5′CAAAGUGGUUGGUGUUUCUUGUGUU3′

TGF-βRII siRNA: 5′AACACAACGUAGCACAGUUGCACCA3′

CII: 5′UGGCAACGUGUCAUCGUUGUGUGUU3′

Results

DIFFERENT GENE-EXPRESSION PATTERNS WERE ASSOCIATED WITH LANDMARK DEVELOPMENTAL STAGES

To identify candidate pathways underlying the developmental processes during BA, we analyzed sea lamprey hepatobiliary transcriptomes at four landmark stages: M0 (National Center for Biotechnology Information Sequence Read Archive database accession number SRX2721810), M2 (SRX2721809), M5 (SRX2721808), and JV (SRX2721807).[10] We annotated 22,297 genes from the hepatobiliary transcriptome assembly (gene-expression data listed in Supporting Table S1). Genes involved in 336 pathways were differentially expressed during developmental BA. Expressions of genes involved in metabolic and biosynthetic pathways were mostly down-regulated. In contrast, genes involved in the biosynthesis of ansamycins, diseases, or cancer pathways were up-regulated, such as TGF-β, MET, platelet-derived growth factor, sonic hedgehog, fibroblast growth factor receptor 3, and genes for extracellular matrices (ECM) and immune cells (Supporting Fig. S2). Interestingly, genes involved in the hedgehog, p53, phosphatidylinositol-4,5-bisphosphate 3-kinase (PI3K)-Akt, TGF-β, and Wnt signaling pathways were differentially expressed during developmental BA (Figs. 2 and 3), consistent with the genes associated with human BA.[21-24]

DOWN-REGULATION OF PI3K AND UP-REGULATION OF SMAD4 MARKED THE TRANSITION FROM M0 TO M2

We reasoned that differentially expressed genes between M0 and M2 play critical roles in the transition from M0 to M2, that is, the onset of BA. Comparison of M0 and M2 transcriptomes revealed that 99 and 73 genes were expressed at least 2-fold higher at M0 (M0 > M2) and M2 (M0 < M2), respectively. A total of 94 pathways with genes up-regulated at M0 were involved in biosynthesis and cell functions. PI3K appeared in 52 of these 94 pathways, such as erythroblastic leukemia viral oncogene homolog, nuclear factor kappa B (NF-κB), hypoxia inducible factor 1, mammalian target of rapamycin, PI3K-Akt, vascular endothelial growth factor, toll-like receptor, Janus kinase (JAK)-signal transducer and activator of transcription (STAT), tumor necrosis factor, neurotrophin, insulin, estrogen, and prolactin signaling pathways (Supporting Fig. S3). A total of 41 pathways with genes up-regulated at M2 were associated with metabolism and steroid or primary bile acid biosynthesis. SMAD4, a cofactor in TGF-β signaling pathway, appeared in 11 of these 41 pathways, in particular, Wnt, TGF-β, Hippo, and phosphatidylinositol glycan-1-like receptor signaling pathways (Supporting Fig. S4). It appeared that down-regulation of PI3K and up-regulation of SMAD4 marked the transition from M0 to M2.

DOWN-REGULATION OF SMAD4 AND UP-REGULATION OF ECM MARKED THE TRANSITION FROM M2 TO M5

We speculated that differential gene expression was involved in the transition from M2 to M5, that is, biliary degeneration and hepatocyte transformation. A comparison of M2 and M5 transcriptomes revealed that 17 and 38 genes were expressed at least 2-fold higher at M2 (M2 > M5) and M5 (M2 < M5), respectively. SMAD4 appeared in 11 pathways with genes up-regulated at M2, including Wnt, TGF-β,
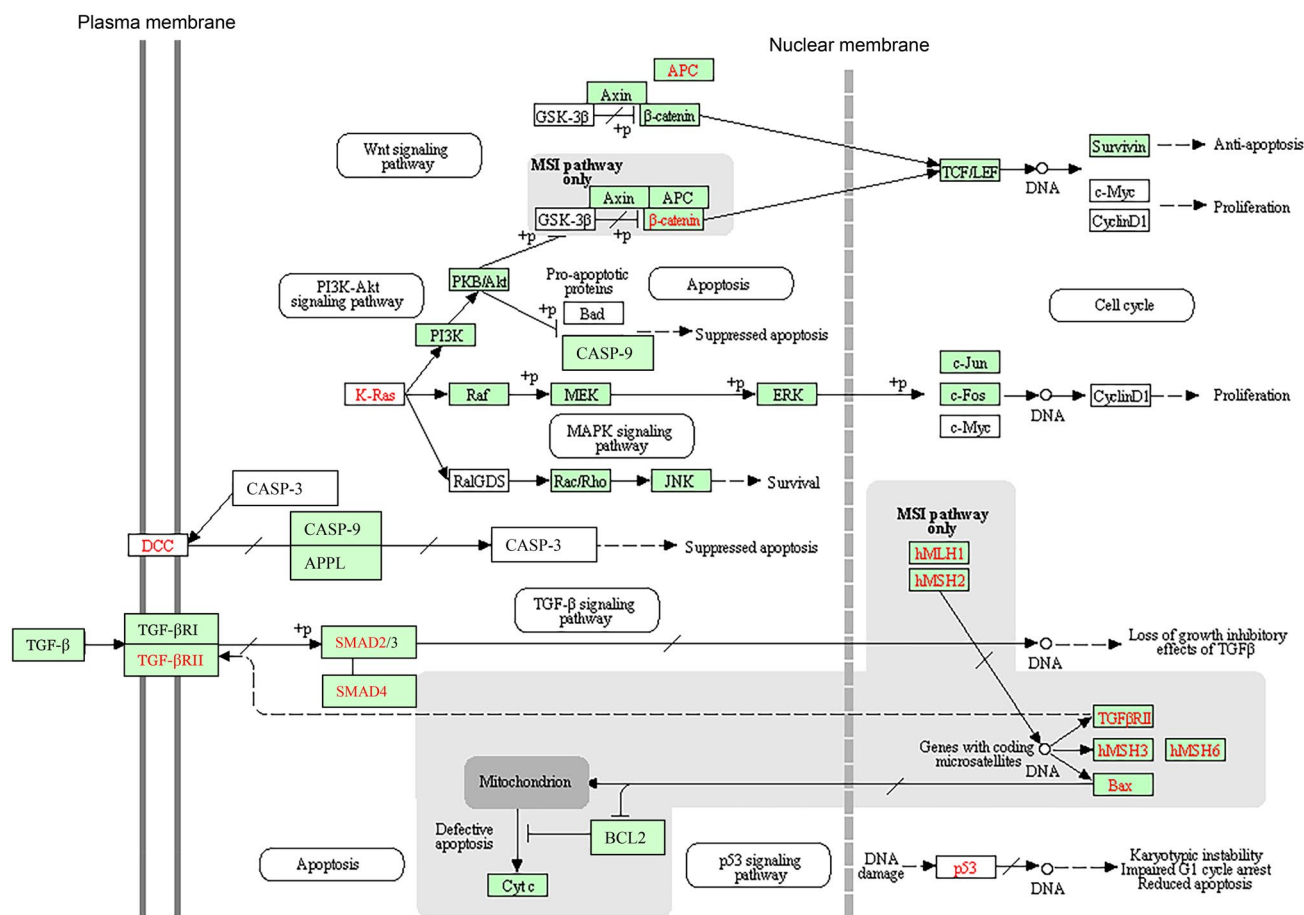
FIG. 2. Genes involved in Wnt, PI3K-Akt, MAPK, TGF-β, microsatellite instability, and p53 signaling pathways were differentially expressed during developmental BA. Hepatobiliary transcriptomes at four landmark stages during developmental BA (M0, M2, M5, and JV) were analyzed with KEGG pathway mapping. Genes up-regulated are highlighted in red, whereas genes down-regulated are highlighted in green. Genes showing both red and green are up-regulated or down-regulated at different developmental stages. Dashed lines represent intermediate signaling steps omitted in the diagram. Abbreviations: APC, adenomatous polyposis coli protein; APPL, adaptor protein, phosphotyrosine interacting with PH domain and leucine zipper 1; Bad, BCL2 associated agonist of cell death; BAX, BCL2 associated X; CASP, caspase; DCC, deleted in colorectal carcinoma; GSK-3β, glycogen synthase kinase 3β; M0, larval stage; LEF, lymphoid enhancer binding factor; M2, metamorphic stage 2; M5, metamorphic stage 5; MSI, microsatellite instability; +p, phosphorylation; RalGDS, Ral guanine nucleotide dissociation stimulator; TCF, transcription factor.

and Hippo signaling pathways (Supporting Fig. S5). A total of 20 pathways contained genes up-regulated at M5, including endocytosis, phagosome, osteoclast differentiation, focal adhesion, ECM receptor interaction, tight junction, leukocyte transendothelial migration, salivary and pancreatic secretions, and disease and cancer pathways (Supporting Fig. S6). Notably, PI3K-AKT, Wnt, Hippo, and insulin-signaling pathways contained genes up-regulated at M5, and ECM genes occurred in 6 of these 20 pathways. It appeared that down-regulation of SMAD4 and up-regulation of ECM marked the transition from M2 to M5.

DOWN-REGULATION OF TGF-βRI AND UP-REGULATION OF MANY OTHER GENES MARKED THE TRANSITION FROM M5 TO JV

We postulated that differential gene expression was involved in the transition from M5 to JV, that is, the completion of BA. Comparison of M5 and JV transcriptomes revealed that 679 and 714 genes were expressed at least 2-fold higher at M5 (M5 > JV) and JV (M5 < JV), respectively. A total of 229 pathways contained genes up-regulated at M5. Among them,
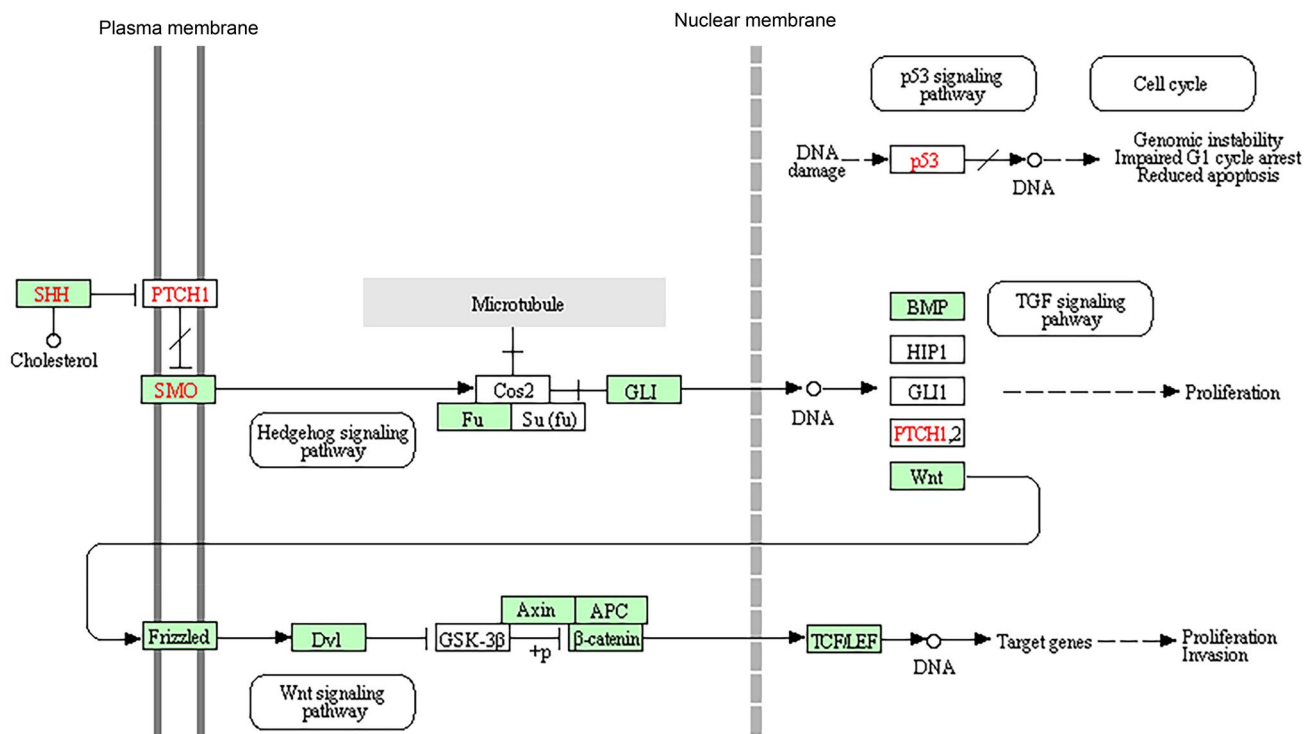
FIG. 3. Genes involved in hedgehog, Wnt, TGF-β, and p53 signaling pathways were differentially expressed during developmental BA. Hepatobiliary transcriptomes at four landmark stages during developmental BA (M0, M2, M5, and JV) were analyzed with KEGG pathway mapping. Genes up-regulated are highlighted in red, whereas genes down-regulated are highlighted in green. Genes showing both red and green are up-regulated or down-regulated at different developmental stages. Dashed lines represent intermediate signaling steps omitted in the diagram. Abbreviations: APC, adenomatous polyposis coli protein; BMP, bone morphogenetic protein; Dvl, disheveled; GSK-3β, glycogen synthase kinase 3β; LEF, lymphoid enhancer binding factor; M0, larval stage; M2, metamorphic stage 2; M5, metamorphic stage 5; $^+$p, phosphorylation; PTCH, patched; SHH, sonic hedgehog; SMO, smoothened; TCF, transcription factor.

the PI3K regulatory subunit appeared in 50, phospholipase C in 26, G-protein $G_{i/o}$ in 18, insulin in 11, and TGF-βRI in 11 pathways, respectively. A total of 239 pathways contained genes up-regulated at JV. Among them, the PI3K catalytic subunit appeared in 51, NF-κB in 37, inhibitor of NF-κB in 26, p38 in 20, cyclic adenosine monophosphate response element-binding protein in 16, caspases in 15, STAT in 14, and calmodulin in 12 pathways, respectively. It appeared that the transition from M5 to JV (completion of BA) was marked by the down-regulation of insulin and TGF-βRI signaling pathways and up-regulation of PI3K-related pathways.

TRANSCRIPTOMIC DIFFERENCES BETWEEN M0 AND JV

After metamorphosis, the transformed JV is manifestly different from the larvae externally and internally. We wanted to investigate differential gene expressions in lamprey with and without bile ducts and compared the hepatobiliary transcriptomes at M0 and JV. A total of 660 genes were up-regulated in M0, and 722 genes were up-regulated in JV among 299 pathways. Metabolism shifted from predominantly biosynthetic in larvae to predominantly catabolic in JVs. However, biosynthesis of steroid, streptomycin, heparin sulfate/heparin, terpenoid backbone, sesquiterpenoid, triterpenoid, and unsaturated fatty acid were up-regulated in JVs (Supporting Fig. S7). Genes involved in different DNA repair mechanisms, cell cycle, vesicle transport, MAPK, Notch, and JAK-STAT signaling pathways, as well as olfactory transduction, were also up-regulated in JVs (Supporting Fig. S8). These changes probably reflect the different metabolic needs of sedentary benthic filter feeding larvae compared with blood-sucking aductal ductal JVs.

TGF-β SIGNALING PATHWAY IS CRITICAL DURING GB DEGENERATION

Because SMAD4, a universal cofactor of TGF-β signaling, was up-regulated at M2 and down-regulated at M5, and TGF-βRI was down-regulated at JV, we posited that TGF-β signaling was important during developmental BA. Therefore, we monitored messenger RNA (mRNA) concentrations of TGF-β1, TGF-β2, and their receptors TGF-βRI and TGF-βRII at stages M0, M1-M7, and JV. Quantitative RT-PCR revealed that transcripts of ligand-binding TGF-βRII peaked at the onset of metamorphosis (*M1; Fig. 4), whereas TGF-β1 and TGF-β2 peaked at M3 (the stage with heightened bile duct degeneration (Fig. 4). Notably, the gene expression of each TGF-β signaling component did not synchronize (Fig. 4). However, because we were not able to isolate different cell types for gene-expression studies, we cannot rule out that the changes in gene expression were simply due to the changes in the number of cells that expressed them.
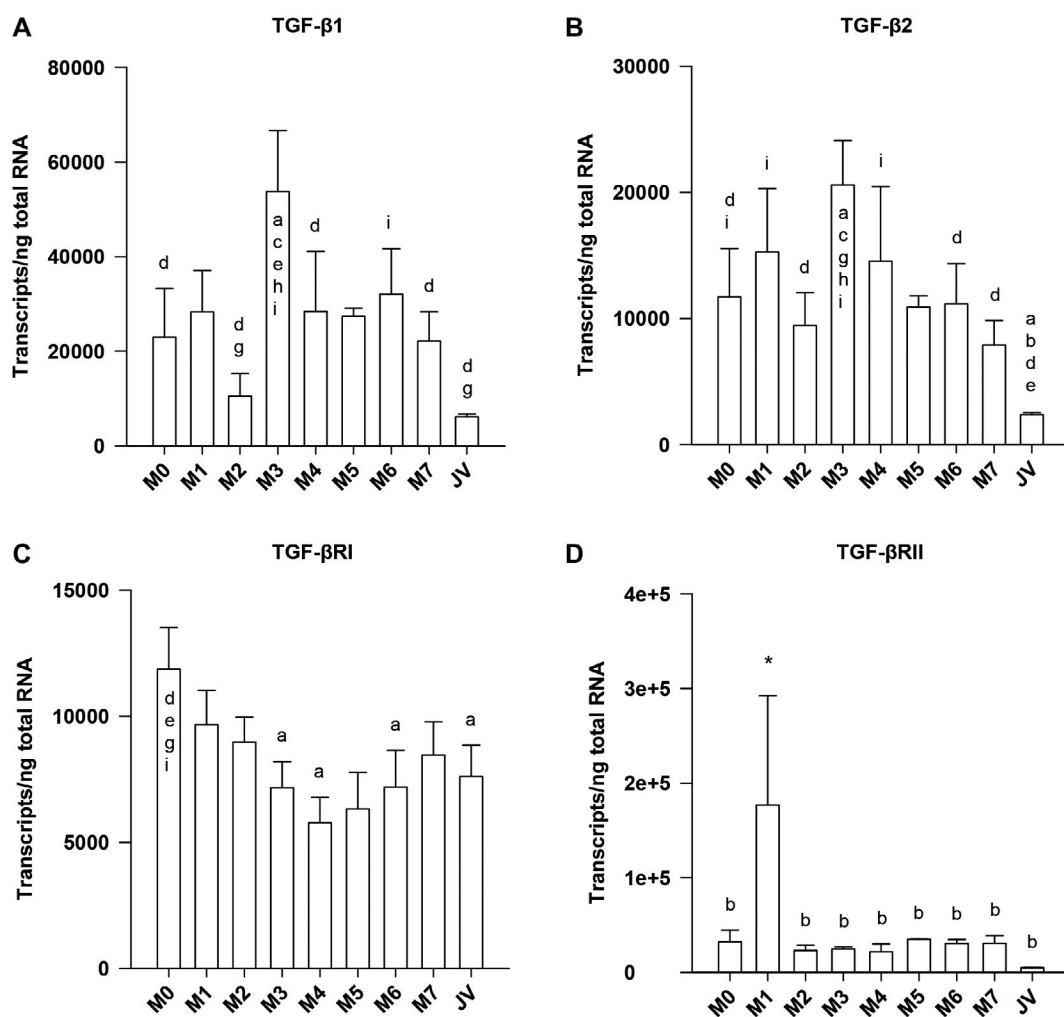
FIG. 4. Hepatobiliary expression of TGF-β-related genes fluctuated at different sea lamprey life stages. Note that the gene-expression patterns of (TGF-β1 (A), TGF-β2 (B), TGF-βRI (C), and TGF-βRII (D) receptors were not in sync. Quantitative data were analyzed using analysis of variance followed by *post hoc* tests when $P < 0.05$. Bar graphs represent mean ± SEM: a, significantly different from M0 (n = 10); b, significantly different from M1 (n = 4); c, significantly different from M2 (n = 12); d, significantly different from M3 (n = 8); e, significantly different from M4 (n = 6); f, significantly different from M5 (n = 2); g, significantly different from M6 (n = 6); h, significantly different from M7 (n = 6); and i, significantly different from JV (T, n = 5). *Significantly different from all other stages. Abbreviations: 1e+5, 1,00,000; M0, larval stage; M1-M7, metamorphic stages 1-7.

T/SRE PREVAILED IN GENES DIFFERENTIALLY EXPRESSED DURING DEVELOPMENTAL BA

To evaluate the potential impact of TGF-β signaling during developmental BA, we examined the number of genes containing T/SRE in hepatobiliary transcriptomes (Supporting Tables S9 and S10). In the sea lamprey genome,[12] T/SRE sequences were found in coding regions of 494 genes (Supporting Table S9) and promoter regions of 180 genes (Supporting Table S10). A total of 400 of the genes containing T/SRE sequences in coding regions and 120 of the genes containing T/SRE sequences in promoter regions were differentially expressed in the hepatobiliary transcriptomes during developmental BA (Supporting Tables S9 and S10). As expected, these genes were involved in TGF-β self-regulation, bile formation and reabsorption, apoptosis, fibrosis, and cholestasis during developmental BA (Supporting Tables S9 and S10).

DISRUPTING TGF-βRI DELAYED GB DEGENERATION

Because GB degeneration is the major event at M2, and SMAD4, a universal cofactor of the TGF-β signaling pathway, was up-regulated at M2, we examined whether disrupting TGF-β signaling at M2 would affect GB degeneration. We inhibited TGF-βRI kinase activity with an antagonist, SJN2511, which stalled metamorphosis before M3 (χ^2 = 17.351; degrees of freedom [DF] = 6; P = 0.0081; Fig. 5A) and delayed GB degeneration (χ^2 = 80, DF = 1, P < 0.0001; Fig. 5B). In addition, the average GB diameter was 19% larger (control: 2.396 ± 0.166 mm, SJN2511: 2.781 ± 0.142 mm; Mann-Whitney U test, P = 0.0365; Fig. 5C). It is worth noting that some SJN2511-treated larvae contained clear GB, similar to some cases of human cystic BA.[4] SJN2511 treatment increased the mRNA levels of TGF-βRII (t test, P = 0.0031), SMAD2 (t test, P = 0.0042), and SMAD3 (t test, P = 0.0337) (Fig. 5D). It appeared that gene expressions of TGF-β signaling components were interactive, and disrupting one component had rippling effects on the other components of the pathway.

In addition, the mRNA levels of CYP7A1 (t test, P = 0.028; Fig. 6) and CYP27A1 (F test, P < 0.0001; Fig. 6), the rate-limiting enzymes for

bile acid biosynthesis, were induced as a result of SJN2511 treatment. However, SJN2511 did not change the overall bile acid pool (control: 1076.407 ± 91.184 ng/mg liver tissue, SJN2511: 989.026 ± 72.773 ng/mg liver tissue; t test, P > 0.05). In addition, gene expressions of the apoptosis-related gene caspase-7 (t test, P = 0.0051) were increased, but MET (t test, P = 0.0492) and NOS2 (t test, P = 0.0272) mRNA levels were decreased (Fig. 6).

PERTURBING TGF-β1 OR TGF-βRII RESULTED IN DISTINCTIVE BILIARY PHENOTYPES

To further investigate the roles of TGF-β signaling pathway on biliary degeneration, we used siRNA to perturb the gene expression of TGF-β1 or TGF-βRII at M2. Disrupting these two TGF-β signaling components resulted in distinctive biliary phenotypes (Fig. 7A,B). TGF-β1 siRNA delayed degeneration of the IHBDs (Fig. 7C; overall χ^2 = 8.217, DF = 2, P = 0.0164, compared with vehicle χ^2 = 5.6, DF = 1, P = 0.018) but not the EHBD (Fig. 7C; same as vehicle), common bile duct (CBD, overall χ^2 = 5.018, DF = 2, P = 0.0813), or the GB (χ^2 = 2.055, DF = 2, P = 0.3579). In contrast, TGF-βRII siRNA delayed the degeneration of EHBD compared with vehicle (χ^2 = 4.286, DF = 1, P = 0.0384; Fig. 7C) but not the IHBD compared with vehicle (χ^2 = 0.171, DF = 1, P = 0.6788; Fig. 7C), CBD compared with vehicle χ^2 = 0.171, DF = 1, P = 0.6788), or GB compared with vehicle (χ^2 = 0.114, DF = 1, P = 0.7353). It appeared that TGF-β1 was essential in degeneration of the IHBD, whereas TGF-βRII was essential in degeneration of the EHBD. Notably, both siRNAs only slightly reduced their respective target gene expressions (11% for TGF-β1 siRNA and 19% for TGF-βRII siRNA; Supporting Fig. S11), but other components in the TGF-β signaling pathway were also affected. TGF-β1 siRNA decreased gene expressions of TGF-β2, TGF-βRI, and TGF-βRII (29%, 32%, and 14%, respectively; Supporting Fig. S11). On the other hand, TGF-βRII siRNA decreased TGF-β1 and TGF-βRI gene expressions by 11% and 9%, respectively, but increased TGF-β2 gene expression by 20% (Supporting Fig. S11). Relatively mild perturbation of the expression of individual genes in the TGF-β signaling pathway affected the expression of multiple other genes, and the entire pathway operated
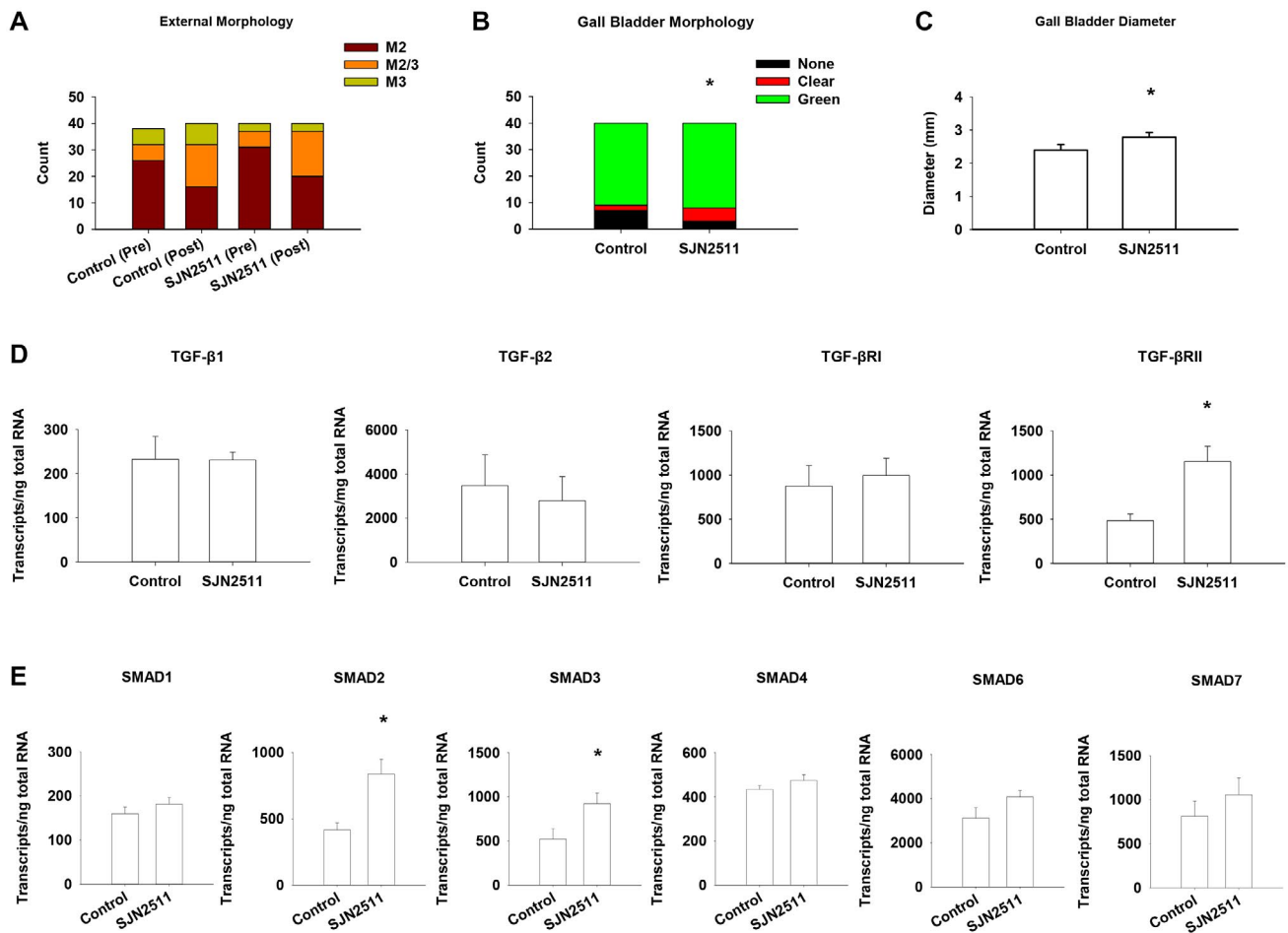
FIG. 5. Disrupting TGF-βRI with antagonist SJN2511 delayed GB degeneration and affected other components of the TGF-β pathway. (A) SJN2511 treatment stalled metamorphosis before metamorphic stage 3 (M3; DF = 6, χ^2 = 18.906, P = 0.0043). (B) SJN2511 treatment delayed GB degeneration (combined green and clear GBs as no degeneration group; DF = 1, χ^2 = 80, P < 0.0001). It was noted that SJN2511-treated lamprey had clear GBs, similar to the clear GB observed in some human cystic BA.[4] (C) The average GB diameter is larger in the SJN2511 treatment group compared with the control (119% of control GB diameter; Mann-Whitney U test, P = 0.0365). (D) SJN2511 treatment increased TGF-βRII mRNA level (t test, P = 0.0031). (E) SJN2511 treatment increased SMAD2 (t test, P = 0.0042) and SMAD3 (t test, P = 0.0337) mRNA levels. *Significantly different from the control group (P < 0.05).

under tight transcriptional control. Subtle changes in any gene we studied caused rippling effects on the entire TGF-β signaling pathway. These results were consistent with the results from the SJN2511 antagonist experiment and the literature on TGF-β signaling.[25-27]

Discussion

Our transcriptomic analyses highlighted the involvement of TGF-β signaling during developmental BA. Similarly, TGF-β has been implicated in human BA.[27,28] TGF-β1 immunoreactive patterns in BA patient were different from that of normal subjects during bile duct development.[28] In normal subjects, TGF-β1 was detected within hepatocytes and ductal plate epithelium from 7 weeks gestation, its immunoreactivity increased within the epithelium of developing bile ducts at 13 weeks' gestation, and apical polarization of TGF-β1 was observed from 16 weeks' gestation. In BA, however, the TGF-β1 immunoreactivity pattern resembled that of the primitive ductal plate at the porta hepatis and within intrahepatic portal tracts, and no significant apical polarization was observed. Therefore, abnormal TGF-β1 expression
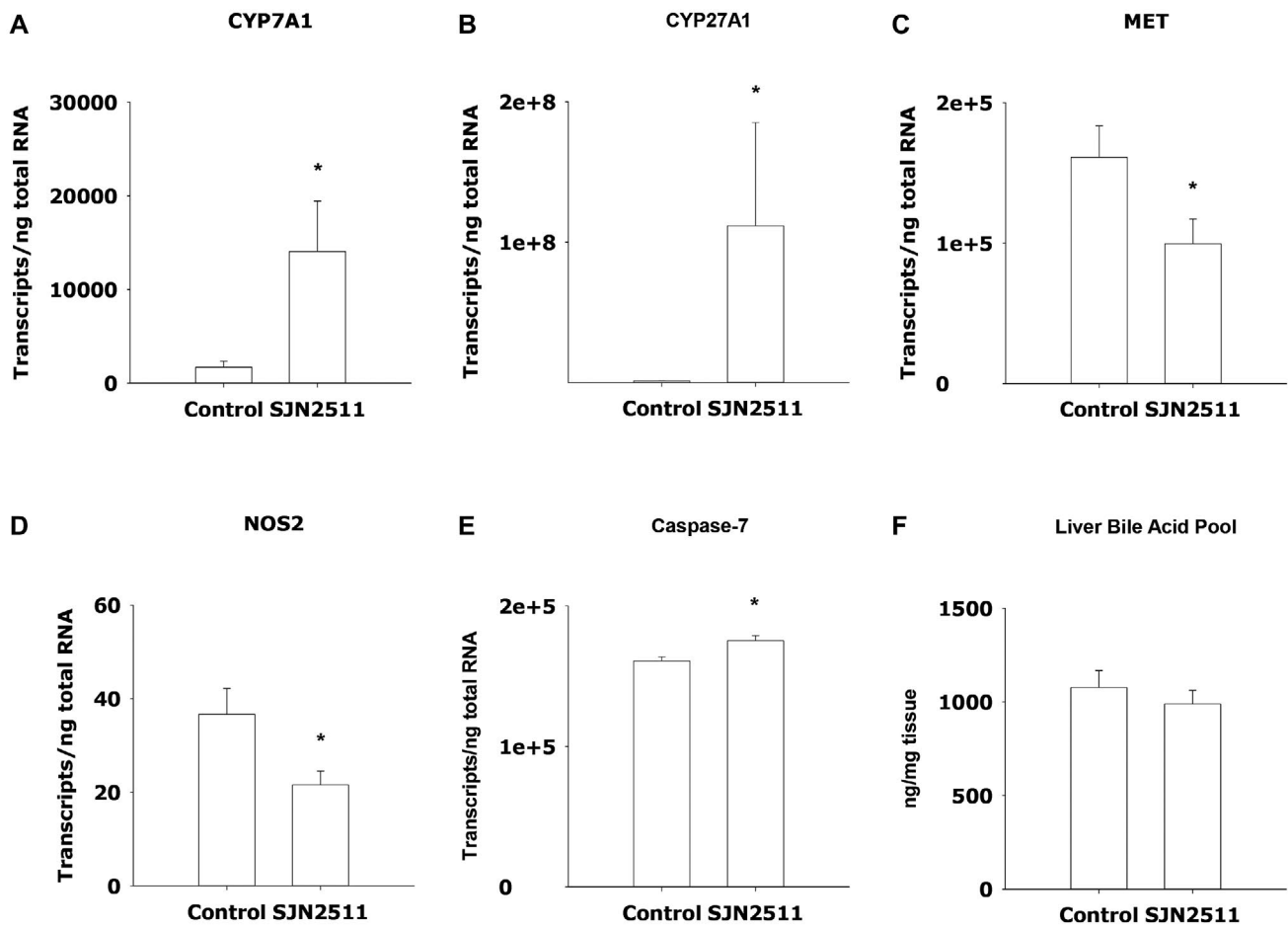
FIG. 6. Disrupting TGF-βRI with antagonist SJN2511 altered the liver gene expressions. SJN2511 increased gene expressions of the rate-limiting enzymes for bile acid biosynthesis CYP7A1 (t test, $P = 0.028$) (A) and CYP27A1 (F test, $P < 0.0001$) (B), and apoptosis-related gene caspase-7 (t test, $P = 0.0051$) (E) but decreased receptor for hepatic growth factor (MET; t test, $P = 0.0492$) (C) and NOS2 (inducible nitric oxide synthase 2; t test, $P = 0.0272$) (D). (F) SJN2511 did not change the level of overall bile acid pool. *Significantly different from the control group ($P < 0.05$). Control group: n = 10; SJN2511 group: n = 9. Abbreviations: 1e+5, 1,00,000; 1e+8, 1,00,000,000.

pattern is associated with developmental arrest in the normal ductal plate remodeling process during BA and may underlie an epithelial-mesenchymal interactive disorder.[28] TGF-β also plays important roles in the fibrogenesis of BA.[29,30]

Our results of KEGG analyses are also consistent with known functions of the TGF-β superfamily. These groups of extracellular proteins are involved in many aspects of development. Homodimers or heterodimers of the TGF-β ligands bind to TGF-βRII, which activates TGF-βRI kinase activity, subsequently activating a network of SMAD proteins and transducing the signal from the cytoplasm to the nucleus. The SMAD proteins can be divided into three groups: receptor-specific SMAD (R-SMAD), common SMAD (Co-SMAD), and inhibitory SMAD (I-SMAD). The R-SMAD group includes SMAD1, 2, 3, 5, and 8. It is worth noting that we did not find SMAD5 in the sea lamprey genome assembly.[11] SMAD4, the universal Co-SMAD, forms a heteromeric complex with the R-SMADs once they are phosphorylated by TGF-βRI. The R-SMAD/Co-SMAD complex then translocates to the nucleus and associates with other transcription factors to regulate target gene expressions. SMAD6 and SMAD7, members of the I-SMAD group, function in the cytoplasm as negative regulators of the intracellular signal transduction network.[25] TGF-β signaling is important during bile duct development and fibrogenesis,[23,29-34] and our data show that it is pivotal during developmental BA.
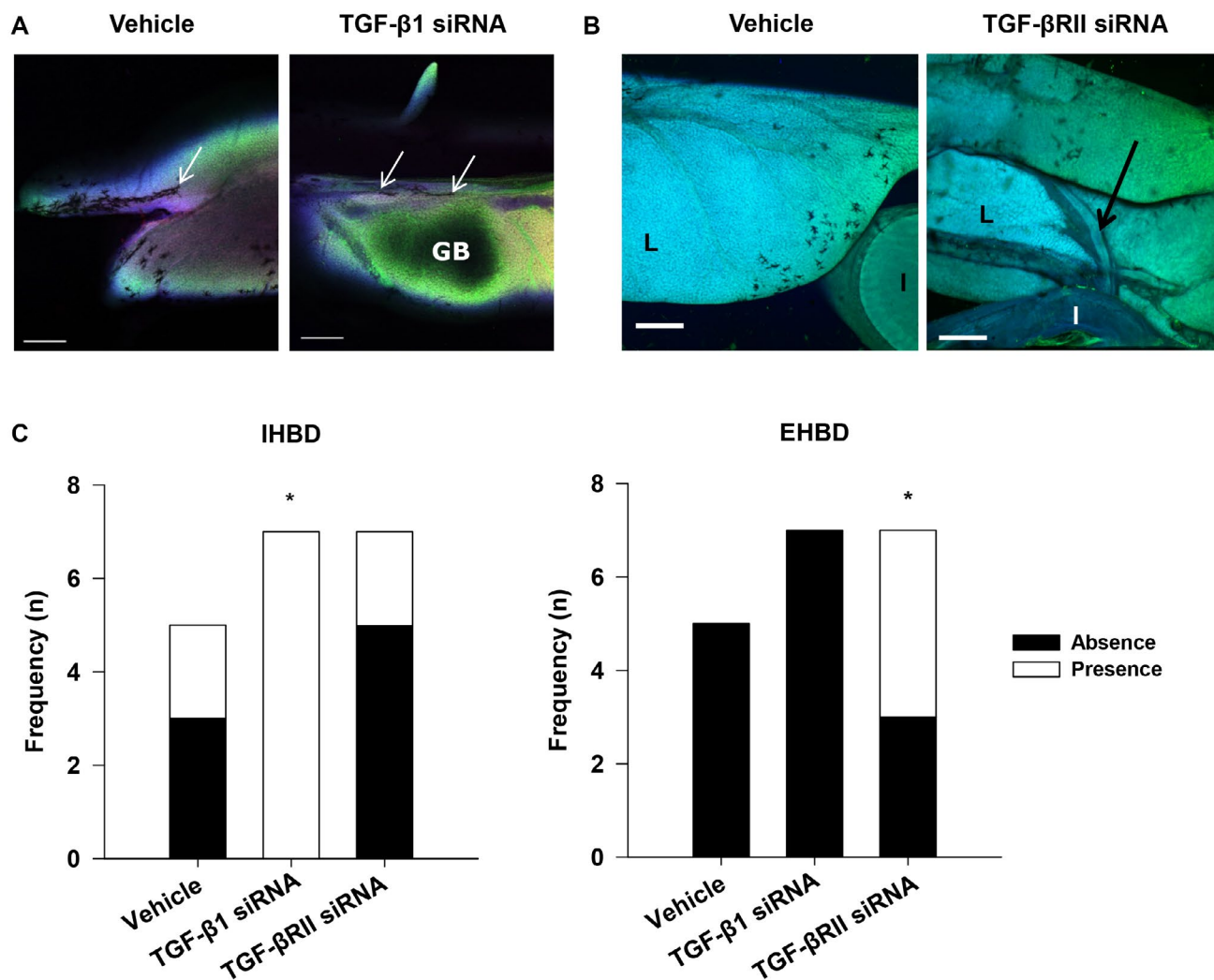
FIG. 7. Perturbation of TGF-β signaling with siRNA delayed biliary degeneration. (A) TGF-β1 siRNA treatment delayed bile duct degeneration. White arrows indicate degenerated bile ducts (blue fluorescence, c-Myc/Alexa 405; green fluorescence, Nissl Green; red fluorescence, TGF-β/Alexa 594). Scale bar: 500 μm. (B) TGF-βRII siRNA treatment delayed extrahepatic bile duct (black arrow) degeneration. Three-dimensional images were reconstructed from confocal Z-serial images of CK19/Alexa 405 (blue) and BCL2/Alexa 488 (green). Scale bar: 500 μm. (C) TGF-β-related siRNA decreased biliary degeneration 2 weeks after treatment: IHBD (χ^2 = 8.217, DF = 2, P = 0.0164) and EHBD (χ^2 = 8.686, DF = 2, P = 0.013). Stacked bar stratified by number of animals in which bile ducts were absent (solid) or present (open), respectively; y-axis maximum corresponds to the total number of animals in each group. *Significantly different from the other groups (P < 0.05).

Disrupting the TGF-β signaling pathway delayed biliary degeneration during developmental BA, supporting the hypothesis generated from our transcriptome analyses that TGF-β signaling is critical for the process of bile duct degeneration. This is consistent with reports that TGF-β1 represses the expression of TGF-βRII during biliary differentiation and development,[28] different affinities and temporal distributions of TGF-β isoforms, and spatially constrained gradients or patterns that characterize the action of TGF-β during development.[26,35,36] Different components of TGF-β signaling are likely involved in distinctive processes during developmental BA, supported by the notion that members of the TGF-β family serve different functions in early embryogenesis versus postembryonic development.[37,38] Impeding TGF-β signaling at critical periods during development, especially TGF-βRII, may prevent the loss

231

of the extrahepatic biliary system and, by extension, BA.[1]

The results of hepatobiliary transcriptome and gene-expression analyses during developmental BA in the sea lamprey are consistent with the notion that the TGF-β signaling pathway plays an important role during programmed cell death,[39] the major process of biliary degeneration during developmental BA,[40] and bile duct tubulogenesis.[31] TGF-β1 appeared to induce apoptosis in areas with rapidly progressing atypical bile duct proliferation.[41] Interestingly, the expression patterns of TGF-βRII during bile duct tubulogenesis in mice is highly dynamic but transient,[31] similar to our gene-expression results throughout the developmental stages. TGF-βRII is expressed in all biliary precursor cells in the ductal plate but is only detectable on the parenchymal side and not on the portal side of the primitive ductal structures. In mature bile ducts, all biliary cells are TGF-βRII-negative. Furthermore, TGF-β1 represses the expression of TGF-βRII, and its distribution was spatially and temporally confined during bile duct development. Sequentially, TGF-β1 first appears uniformly in the cytoplasm of biliary precursor cells and surrounding hepatocytes, then at the portal side, especially the apical margin of the primitive ductal structures, and later in the apical portion of the mature bile ducts.[28] It appears that TGF-β signaling is under tight spatial and temporal control during biliary development and completely shut down when bile ducts are mature.[31] Our gene-expression data were consistent with these findings in that JV (completion of BA) had lowest expression of TGF-β-related genes.

The results of our antagonist and siRNA experiments revealed distinct functions for different TGF-β signaling components. Indeed, different TGF-β isoforms and receptors are expressed in different cell types in human BA and during liver regeneration in rats.[30,33] In normal liver, TGF-β1 and TGF-β2 levels were relatively high in sinusoidal endothelial cells and Kupffer cells, whereas TGF-βRI and TGF-βRII were more abundant in cholangiocytes and hepatocytes. After partial hepatectomy in rats, an early peak of TGF-β2 and TGF-β3 were present in hepatocytes, sinusoidal endothelial cells, Kupffer cells, and stellate cells. Afterward, only hepatocytes showed sustained increase in TGF-β1, TGF-β2, and TGF-β3 mRNA levels. On the other hand, TGF-β mRNA or immunoreactivity were only increased in stellate cells during bile duct ligation–induced fibrosis or in activated fibroblasts/myofibroblasts during early stage of BA, whereas TGF-βRI or TGF-βRII immunoreactivities showed differential decreases among different cell types.[30,33] Therefore, different TGF-β isoforms or receptors were induced in specific cell types for selective mechanisms.[33]

Interestingly, knocking out different TGF-β isoforms resulted in different phenotypes in mice. On a mixed genetic background, approximately 50% $Tgfb1^{-/-}$ conceptuses die midgestation from defective yolk sac vasculogenesis. The other half are developmentally normal but die 3 weeks post partum.[42] TGF-β2 knockout mice have multiple developmental defects that are nonoverlapping with TGF-β1 or TGF-β3 knockout phenotypes.[43] In addition, the expression pattern of a gene in the TGF-β superfamily transduction cascade does not necessarily predict its *in vivo* function.[25] Our results also showed that TGF-β signaling was under stringent self-regulation, and subtle differences in the equilibrium could alter the fate of bile duct degeneration.

Several genome-wide studies of single-nucleotide polymorphisms or copy number variations and cDNA microarray studies in BA patients have associated few susceptible genes with this disease.[23,44-48] For example, adducin 3, ADP ribosylation factor 6, ECM-related genes, endothelial growth factor containing fibulin extracellular matrix protein 1, glypican 1, x-prolyl aminopeptidase 1, and genes for several transcription factors are associated with both embryonic and perinatal BA. Working alone, these genetic variants may not be sufficient to cause BA and may involve other yet-to-be-determined genes.[46] With transcriptome KEGG analyses, we were able to identify additional signaling pathways involved in BA processes. We noticed that the Wnt signaling pathway was down-regulated, whereas the hedgehog signaling pathway was up-regulated in hepatobiliary transcriptomes during developmental BA. These results are consistent with reports that the Wnt/β-catenin pathway supports biliary differentiation in fetal liver explants,[49] and activation of the hedgehog pathway promotes fibrogenesis during BA.[22,50] Therefore, a network of signaling pathways coordinates with the TGF-β pathway to control hepatobiliary differentiation[35] and likely biliary degeneration during developmental BA.

To summarize, TGF-β signaling plays an important role in developmental BA and biliary degeneration.

REFERENCES

1) Petersen C, Davenport M. Aetiology of biliary atresia: what is actually known? Orphanet J Rare Dis 2013;8:128.

2) Haber BA, Russo P. Biliary atresia. Gastroenterol Clin North Am 2003;32:891-911.

3) Berauer JP, Mezina AI, Okou DT, Sabo A, Muzny DM, Gibbs RA, et al. Identification of polycystic kidney disease 1 like 1 gene variants in children with biliary atresia splenic malformation syndrome. Hepatology 2019;70:899-910.

4) De Matos V, Erlichman J, Russo PA, Haber BA. Does "cystic" biliary atresia represent a distinct clinical and etiological subgroup? A series of three cases. Pediatr Dev Pathol 2005;8:725-731.

5) Shen O, Sela HY, Nagar H, Rabinowitz R, Jacobovich E, Chen D, et al. Prenatal diagnosis of biliary atresia: a case series. Early Hum Dev 2017;111:16-19.

6) Sidon EW, Youson JH. Morphological changes in the liver of the sea lamprey, *Petromyzon marinus* L., during metamorphosis. I: Atresia of the bile ducts. J Morphol 1983;177:109-124.

7) Youson JH, Potter IC. A description of the stages in the metamorphosis of the anadromous sea lamprey, *Petromyzon marinus* L. Can J Zool 1979;57:1808-1817.

8) Youson JH, Sidon EW. Lamprey biliary atresia: first model system for the human condition? Experientia 1978;34:1084-1086.

9) Youson JH, Connelly KL. Development of longitudinal mucosal folds in the intestine of the anadromous sea lamprey, *Petromyzon marinus* L., during metamorphosis. Can J Zool 1978;56:2364-2371.

10) Chung-Davidson YW, Yeh CY, Bussy U, Li K, Davidson PJ, Nanlohy KG, et al. Hsp90 and hepatobiliary transformation during sea lamprey metamorphosis. BMC Dev Biol 2015;15:47.

11) Smith JJ, Kuraku S, Holt C, Sauka-Spengler T, Jiang N, Campbell MS, et al. Sequencing of the sea lamprey (*Petromyzon marinus*) genome provides insights into vertebrate evolution. Nat Genet 2013;45:415-421, e411-e412.

12) Trapnell C, Pachter L, Salzberg SL. TopHat: discovering splice junctions with RNA-seq. Bioinformatics 2009;25:1105-1111.

13) Trapnell C, Roberts A, Goff L, Pertea G, Kim D, Kelley DR, et al. Differential gene and transcript expression analysis of RNA-seq experiments with TopHat and Cufflinks. Nat Protoc 2012;7:562-578.

14) Du Z, Zhou X, Ling Y, Zhang Z, Su Z. AgriGO: a GO analysis toolkit for the agricultural community. Nucleic Acids Res 2010;38:W64-W70.

15) **Tian T**, **Liu Y, Yan H**, You Q, Yi X, Du Z, et al. AgriGO v2.0: a GO analysis toolkit for the agricultural community, 2017 update. Nucleic Acids Res 2017;45:W122-W129.

16) **Stopa M**, **Anhuf D**, Terstegen L, Gatsios P, Gressner AM, Dooley S. Participation of Smad2, Smad3, and Smad4 in transforming growth factor beta (TGF-beta)-induced activation of Smad7: the TGF-beta response element of the promoter requires functional Smad binding element and E-box sequences for transcriptional regulation. J Biol Chem 2000;275:29308-29317.

17) Lin G, Gai R, Chen Z, Wang Y, Liao S, Dong R, et al. The dual PI3K/mTOR inhibitor NVP-BEZ235 prevents epithelial-mesenchymal transition induced by hypoxia and TGF-beta1. Eur J Pharmacol 2014;729:45-53.

18) Yang X, Hou F, Taylor L, Polgar P. Characterization of human cyclooxygenase 2 gene promoter localization of a TGF-beta response element. Biochim Biophys Acta 1997;1350:287-292.

19) Li K, Scott AM, Chung-Davidson YW, Bussy U, Patel T, Middleton ZE, et al. Quantification of oxidized and unsaturated bile alcohols in sea lamprey tissues by ultra-high performance liquid chromatography-tandem mass spectrometry. Molecules 2016;24:1119.

20) Chung-Davidson YW, Davidson PJ, Scott AM, Walaszczyk EJ, Brant CO, Buchinger T, et al. A new clarification method to visualize biliary degeneration during liver metamorphosis in sea lamprey (*Petromyzon marinus*). J Vis Exp 2014;88:e51648.

21) Girard M, Panasyuk G. Genetics in biliary atresia. Curr Opin Gastroenterol 2019;35:73-81.

22) **Omenetti A**, **Bass LM**, Anders RA, Clemente MG, Francis H, Guy CD, et al. Hedgehog activity, epithelial-mesenchymal transitions, and biliary dysmorphogenesis in biliary atresia. Hepatology 2011;53:1246-1258.

23) Chen L, Goryachev A, Sun J, Kim P, Zhang H, Phillips MJ, et al. Altered expression of genes involved in hepatic morphogenesis and fibrogenesis are identified by cDNA microarray analysis in biliary atresia. Hepatology 2003;38:567-576.

24) Choe BH, Kim KM, Kwon S, Lee KS, Koo JH, Lee HM, et al. The pattern of differentially expressed genes in biliary atresia. J Korean Med Sci 2003;18:392-396.

25) Chang H, Lau AL, Matzuk MM. Studying TGF-beta superfamily signaling by knockouts and knockins. Mol Cell Endocrinol 2001;180:39-46.

26) Clotman F, Jacquemin P, Plumb-Rudewiez N, Pierreux CE, Van der Smissen P, Dietz HC. Control of liver cell fate decision by a gradient of TGF beta signaling modulated by Onecut transcription factors. Genes Dev 2005;19:1849-1854.

27) Iordanskaia T, Hubal MJ, Koeck E, Rossi C, Schwarz K, Nadler EP. Dysregulation of upstream and downstream transforming growth factor-beta transcripts in livers of children with biliary atresia and fibrogenic gene signatures. J Pediatr Surg 2013;48:2047-2053.

28) Tan CEL, Chan VSW, Yong RYY, Vijayan V, Tan WL, Fook Chong SMC, et al. Distortion in TGFβI peptide immunolocalization in biliary atresia: comparison with the normal pattern in the developing human intrahepatic bile duct system. Pathol Int 1995;45:815-824.

29) Lee SY, Chuang JH, Huang CC, Chou MH, Wu CL, Chen CM, et al. Identification of transforming growth factors actively transcribed during the progress of liver fibrosis in biliary atresia. J Pediatr Surg 2004;39:702-708.

30) Ahmed A, Ohtani H, Nio M, Funaki N, Iwami D, Kumagai S, et al. In situ expression of fibrogenic growth factors and their receptors in biliary atresia: comparison between early and late stages. J Pathol 2000;192:73-80.

31) Lemaigre FP. Molecular mechanisms of biliary development. In: Kaestner KH, ed. Development, Differentiation and Disease of the Para-Alimentary Tract. Vol. 97. San Diego, CA: Elsevier Academic Press, Inc.; 2010:103-126.

32) Wang W, Feng Y, Aimaiti Y, Jin X, Mao X, Li D. TGFbeta signaling controls intrahepatic bile duct development may through regulating the Jagged1-Notch-Sox9 signaling axis. J Cell Physiol 2018;233:5780-5791.

33) Bissell DM, Wang SS, Jarnagin WR, Roll FJ. Cell-specific expression of transforming growth-factor-beta in rat-liver—evidence for autocrine regulation of hepatocyte proliferation. J Clin Invest 1995;96:447-455.

34) Glaser SS, Gaudio E, Miller T, Alvaro D, Alpini G. Cholangiocyte proliferation and liver fibrosis. Expert Rev Mol Med 2009;11:e7.

35) Clotman F, Lemaigre WP. Control of hepatic differentiation by activin/TGF beta signaling. Cell Cycle 2006;5:168-171.

36) Zong Y, Stanger B-Z. Molecular mechanisms of bile duct development. Int J Biochem Cell Biol 2011;43:257-264.

37) Green JBA, Smith JC. Growth factors as morphogens: do gradients and thresholds establish body plan? Trends Genet 1991;7:245-250.

38) Wilkins A, Gubb D. Pattern formation in embryo and imaginal discs of Drosophila: what are the links? Dev Biol 1991;145:1-12.

39) Kanzler S, Galle PR. Apoptosis and the liver. Semin Cancer Biol 2000;10:173-184.

40) Boomer LA, Bellister SA, Stephenson LL, Hillyard SD, Khoury JD, Youson JH, et al. Cholangiocyte apoptosis is an early event during induced metamorphosis in the sea lamprey, *Petromyzon marinus* L. J Pediatr Surg 2010;45:114-120.

41) Takiya S, Tagaya T, Takahashi K, Kawashima H, Kamiya M, Fukuzawa Y, et al. Role of transforming growth factor beta 1 on hepatic regeneration and apoptosis in liver diseases. J Clin Pathol 1995;48:1093-1097.

42) Dickson MC, Martin JS, Cousins FM, Kulkarni AB, Karlsson S, Akhurst RJ. Defective hematopoiesis and vasculogenesis in transforming growth-factor-beta-1 knock out mice. Development 1995;121:1845-1854.

43) Sanford LP, Ormsby I, Gittenberger-de Groot AC, Sariola H, Friedman R, Boivin GP, et al. TGFβ2 knockout mice have multiple developmental defects that are non-overlapping with other TGFβ knockout phenotypes. Development 1997;124:2659-2670.

44) **Chen Y**, **Gilbert MA**, Grochowski CM, McEldrew D, Llewellyn J, Waisbourd-Zinman O, et al. A genome-wide association study identifies a susceptibility locus for biliary atresia on 2p16.1 within the gene *EFEMP1*. PLoS Genet 2018;14:e1007532.

45) **Garcia-Barceló M-M**, **Yeung M-Y**, **Miao X-P**, **Tang CS-M**, Chen G, So M-T, et al. Genome-wide association study identifies a susceptibility locus for biliary atresia on 10q24.2. Hum Mol Genet 2010;19:2917-2925.

46) Ningappa M, Min J, Higgs BW, Ashokkumar C, Ranganathan S, Sindhi R. Genome-wide association studies in biliary atresia. Wiley Interdiscip Rev Syst Biol Med 2015;7:267-273.

47) Tsai EA, Grochowski CM, Loomes KM, Bessho K, Hakonarson H, Bezerra JA, et al. Replication of a GWAS signal in a Caucasian population implicates *ADD3* in susceptibility to biliary atresia. Hum Genet 2014;133:235-243.

48) Zhang D-Y, Sabla G, Shivakumar P, Tiao G, Sokol RJ, Mack C, et al. Coordinate expression of regulatory genes differentiates embryonic and perinatal forms of biliary atresia. Hepatology 2004;39:954-962.

49) Hussain SZ, Sneddon T, Tan XP, Micsenyi A, Michalopoulos GK, Monga SPS. Wnt impacts growth and differentiation in ex vivo liver development. Exp Cell Res 2004;292:157-169.

50) Omenetti A, Porrello A, Jung Y, Yang L, Popov Y, Choi SS, et al. Hedgehog signaling regulates epithelial-mesenchymal transition during biliary fibrosis in rodents and humans. J Clin Invest 2008;118:3331-3342.

Author names in bold designate shared co-first authorship.

Supporting Information

Additional Supporting Information may be found at onlinelibrary.wiley.com/doi/10.1002/hep4.1461/suppinfo.